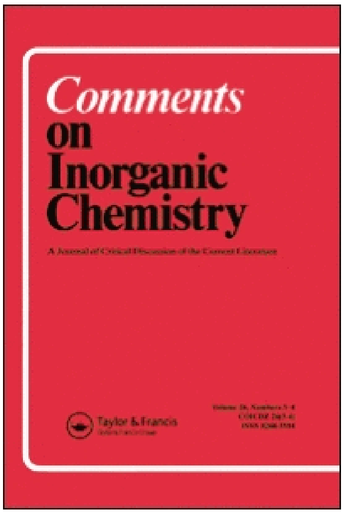

Comments on Inorganic Chemistry

Publication details, including instructions for authors and subscription information:
http://www.informaworld.com/smpp/title~content=t713455155

Electronic Absorption-Ligand-Field Transitions

To cite this Article (1984) 'Electronic Absorption-Ligand-Field Transitions', Comments on Inorganic Chemistry, 3: 5, 238 — 249

To link to this Article: DOI: 10.1080/02603598408080074

URL: http://dx.doi.org/10.1080/02603598408080074

References

1. (a) A. Abragam and B. Bleaney, *Electron Paramagnetic Resonance of Transition Ions* (Oxford University Press, London, 1970).
   (b) J. E. Wertz and J. R. Bolton, *Electron Spin Resonance: Elementary Theory and Practical Applications* (McGraw-Hill, New York, 1972).
   (c) B. R. McGarvey, in *Transition Metal Chemistry,* edited by R. L. Carlin, (Marcel Dekker, New York, 1966).
   (d) E. Konig, in *Physical Methods in Advanced Inorganic Chemistry,* edited by H. A. O. Hill and P. Day (Wiley-Interscience, New York, 1968).
   (e) B. A. Goodman and J. B. Raynor, Adv. Inorg. Chem. Radiochem. **13,** 135 (1970).
   (f) R. S. Drago, *Physical Methods in Chemistry* (Saunders, Philadelphia, 1977).
   (g) A. Bencini and D. Gatteschi, in *Transition Metal Chemistry,* edited by G. A. Melson and B. N. Figgis (Marcel Dekker, New York, 1982).
2. P. Cassidy and M. A. Hitchman, Inorg. Chem. **16,** 1568–1570 1977).
3. C. J. Ballhausen, *Molecular Electronic Structures of Transition Metal Complexes* (McGraw-Hill, New York, 1979).
4. J. H. Van Vleck, *The Theory of Electric and Magnetic Susceptibilities* (Oxford, London, 1965).
5. K. W. Penfield, A. A. Gewirth, E. I. Solomon, manuscript in preparation.
   g values were computed from the wavefunctions given by a SCF-Xα-SW calculation. The wavefunctions formed the basis set for a complete calculation, and the diagonal elements were the observed transition energies. Both ligand-field and charge-transfer states were included in this matrix. The off-diagonal elements were computed through the operation of both ligand and metal spin-orbit coupling on these functions. The matrix was diagonalized and a new, spin-orbit corrected ground state wavefunction was obtained. A g^2 tensor was calculated and the principle g values were obtained. A single parameter was introduced in the original wavefunctions to alter the covalent mixing between metal and ligand components. This parameter was varied to fit the calculated g values to those experimentally observed.

III. ELECTRONIC ABSORPTION—LIGAND-FIELD TRANSITIONS

A. Basic Principles

In EPR spectroscopy we focused on the $^2B_{1g}$ ground state wavefunction. This was accomplished by perturbing it with an external magnetic field and observing transitions between the Zeeman-split ground state components using radiation in the $\sim$0.3 cm^{-1} region. In electronic absorption spectroscopic studies of the ligand-field transitions,[1] we are probing the splittings of all the d orbitals produced by the ligand field. For $CuCl_4^=$, excitation of electrons from the filled d orbitals into the hole in the $b_{1g}(x^2 - y^2)$ orbital produces a number

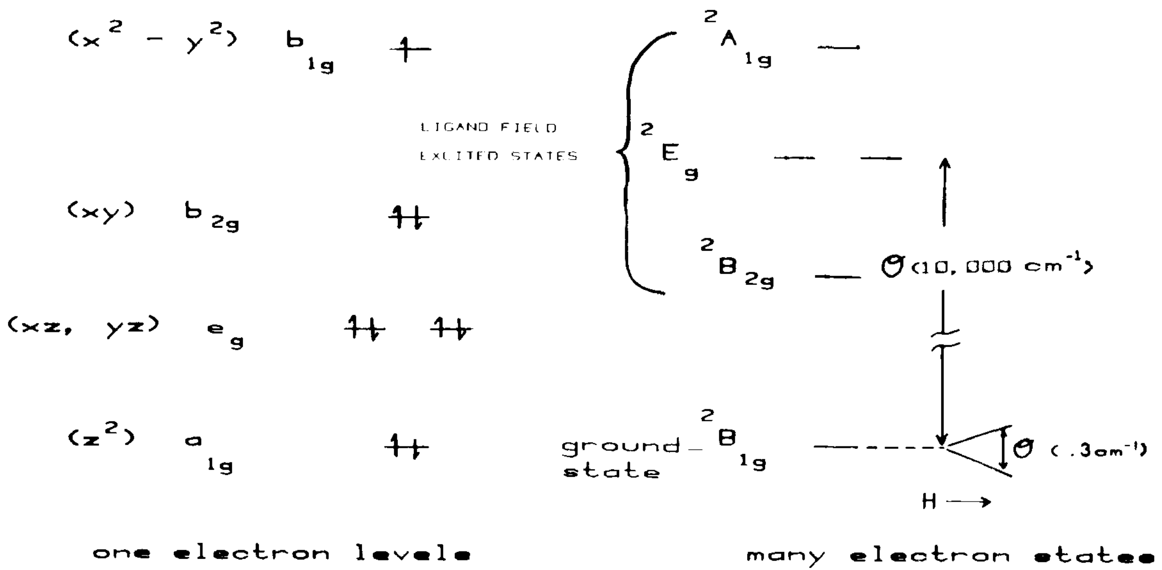

FIGURE III-1 Ligand-field states of D_{4h}–$CuCl_4^{=}$ associated with the square planar splitting of the *d* orbitals.

of $d \rightarrow d$ or ligand-field excited states (shown to the right in Figure III-1). These are on the order of 10,000 cm^{-1} in energy above the ground state, making them accessible by near-IR-VIS-UV radiation.

In electronic absorption spectroscopy we are interested in the interaction of electromagnetic radiation with the complex which produces a transition from the ground state ψ_g to the excited state ψ_e (Figure III-2a). On an experimental level we observe an absorption band associated with this transition (Figure III-2b). The important quantity which enables us to correlate experiment with theory is the oscillator strength f. Experimentally, the oscillator strength is directly related to the area under the absorption band and is given by Eq. (III-1a):

$$f_{\text{exp}} = (4.332 \times 10^{-9}) \int \epsilon(\nu) d\nu \qquad \text{(III-1a)}$$

$$f_{\text{theory}} = (1.085 \times 10^{11}) \, \nu [\textstyle\int \psi_g \hat{M} \psi_e d\tau]^2 \, . \qquad \text{(III-1b)}$$

Theoretically,[2] the oscillator strength is given by Eq. (III-1b) where $\hat{M}$ is the transition moment operator for the interaction of radiation with the electron. For near-IR-VIS-UV radiation, the wavelength of

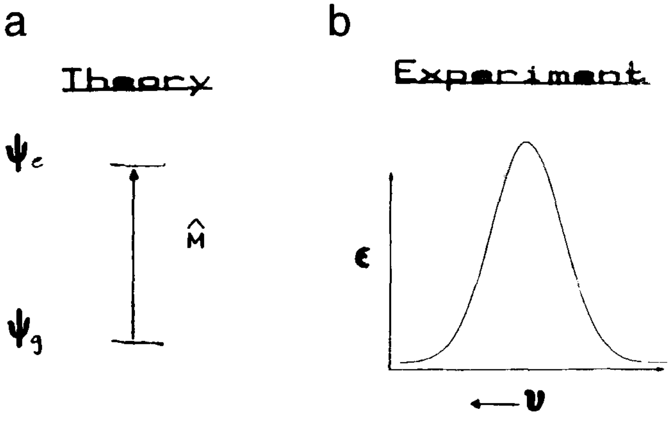

FIGURE III-2 An electronic transition: (a) theory, and (b) experiment.

light is on the order of a few thousand angstroms, which is large relative to the radius of the electron in its orbital. This allows one to express $\hat{M}$ as the multipole expansion given in Eq. (III-2a):

$$\hat{M} = \hat{M}(\text{electric dipole}) + \hat{M}(\text{magnetic dipole}) \tag{III-2a}$$

$$+ \hat{M}(\text{electric quadrupole})$$

$$= \hat{M}(x,y,z) + \hat{M}(R_x, R_y, R_z) \tag{III-2b}$$

$$+ \hat{M}(x^2, xy, y^2, xz, yz, z^2).$$

The dominant term in this expansion is the electric dipole moment operator, $\vec{M}$(electric dipole), which as indicated in Eq. (III-2b) transforms as the electron coordinates x, y, z. Theoretically, the electric dipole component of $d \rightarrow d$ transition intensity in metal complexes is predicted[3] to be $\sim 10^4$ greater than the magnetic dipole component. Experimentally, the latter has only been definitely observed[1b] for the lowest excited state of octahedral Ni(II) and Co(II) complexes. Thus we now consider the electric dipole operator in detail.

From Eqs. (III-1), in order to observe an absorption band, the oscillator strength must be greater than zero. This requires that the integral in Eq. (III-1b), $\int \psi_g \vec{M}(x,y,z) \psi_e d\tau$, must be greater than zero for an "electric dipole allowed" transition. If we first consider the $d \rightarrow d$ transitions in the free metal ion, both the ground and excited states have g symmetry with respect to inversion. Since $\vec{M}(x,y,z)$ has u symmetry, the integral of Eq. (III-1b) has $g \times u \times g = u$ symmetry which requires that the integral must equal zero. Thus, the $d \rightarrow d$ transitions are parity (i.e., inversion) or Laporté forbidden.

This is strictly true for the free ion; however, in a metal complex the ligand field can overcome the parity forbiddenness of the $d \rightarrow d$ transitions in two ways.[4] First for centrosymmetric complexes (i.e., those which possess inversion symmetry), a number of odd parity normal modes of vibration exist which eliminate inversion at the metal ion dynamically during the time course of the vibration. For example, in D_{4h}–$\text{CuCl}_4^=$ the b_{2u} vibration illustrated by the dashed arrows in Figure III-3a produces a dynamic distortion of the complex toward a D_{2d} distorted tetrahedron, which clearly eliminates the inversion symmetry at the copper ion. The Franck-Condon principle

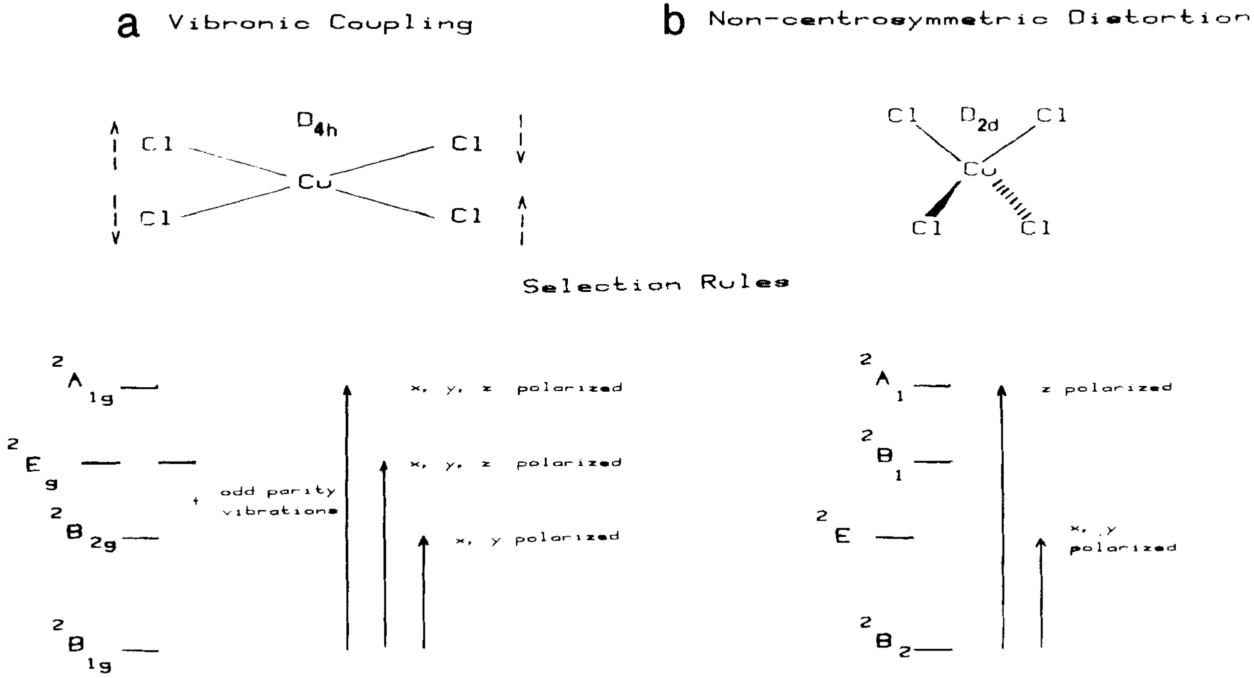

FIGURE III-3 Intensity mechanisms for ligand field transitions in metal complexes: (a) vibronic coupling and (b) noncentrosymmetric distortion.

requires that electronic transitions occur rapidly relative to nuclear motion. Hence, transitions which occur during the b_{2u} vibration experience a ligand field which contains no inversion. This is known as vibronic or Herzberg-Teller coupling and is considered further in Section VIII. In D_{4h}-$CuCl_4^=$ all three $d \rightarrow d$ transitions are made electric dipole allowed by coupling with odd parity vibrations of the square planar complex (Figure III-3a bottom).

The ligand field can also overcome the parity forbiddenness of the $d \rightarrow d$ transitions through a static distortion of the complex which eliminates its inversion symmetry. For a number of counter-ions, $CuCl_4^=$ is found to crystallize in the noncentrosymmetric D_{2d} distorted tetrahedral geometry shown at the top of Figure III-3b. This D_{2d} distortion eliminates the inversion much more effectively than odd parity vibrations due to its static nature. Hence the $d \rightarrow d$ transitions associated with noncentrosymmetric complexes are more intense. The D_{2d} ligand field of $CuCl_4^=$ produces the energy level diagram of the $d \rightarrow d$ transitions shown at the bottom of Figure III-3b (*vide infra*). Note that the ground state of $CuCl_4^=$ transforms as $^2B_2$ in the D_{2d} geometry. One can now use group theory to determine the selection rules associated with $d \rightarrow d$ transitions from this ground state, which are made allowed by the electric dipole moment operator in the integral of Eq. (III-1b). In particular, the $^2B_2 \rightarrow {}^2E$ transition is allowed only for light polarized along the x,y molecular axes and the $^2B_2 \rightarrow {}^2A_1$ transition is allowed for light which is polarized along the z axis of the D_{2d}-$CuCl_4^=$ complex (Figure III-3b, bottom). These selection rules permit a definitive experimental assignment of the absorption spectrum.

It should be emphasized that the actual source of intensity for $d \rightarrow d$ transitions comes from the (dynamic or static) distortion-induced mixing of Laporté-allowed, higher-energy charge-transfer excited states (see Section IV) into the states derived from the pure d orbitals. Thus the distortion can be treated as contributing a new perturbation term to the molecular Hamiltonian ($H'_{\text{odd parity}}$). This leads to a perturbed excited state "d" wavefunction,[5]

$$|\psi_e'\rangle = |\psi_e\rangle + \frac{\langle\psi_e|H'_{\text{odd parity}}|\psi_u\rangle}{E_e - E_u}|\psi_u\rangle \qquad \text{(III-3)}$$

where ψ_u is a higher energy charge-transfer state which is Laporté allowed for a transition from the d orbital ground state ψ_g with an oscillator strength f_u. Substitution of this perturbed excited state wavefunction into Eq. (III-1b) gives

$$f_{g\rightarrow e} = \frac{v_e}{v_u}\left[\frac{\langle\psi_e|H'_{\text{odd parity}}|\psi_u\rangle}{E_e - E_u}\right]^2 f_u . \qquad \text{(III-4)}$$

Thus as the excited state energy E_e becomes closer to the energy of ψ_u (E_u), the intensity increases due to more efficient "intensity borrowing" from the Laporté allowed transition. The ratio of intensities is directly related to the coefficient of mixing in Eq. (III-3). For a static distortion, $H'_{\text{odd parity}}$ can be obtained from ligand-field theory[1a,3] or from configurational interaction in molecular orbital theory. The form of $H'_{\text{odd parity}}$ for vibronic coupling is discussed in Section VIII.

B. The Experiment

The electronic absorption spectrum of a solution or frozen glass of $CuCl_4^=$ results from an average over all possible projections of the $\vec{E}$ vector of light onto the molecular axes of the complex. Alternatively, one can polarize the light and propagate it through a single crystal containing the $CuCl_4^=$ complex with a crystallographically defined orientation of the molecular axes. The polarized single crystal absorption spectrum obtained from this experiment allows a direct determination of the selection rules for a given absorption band, hence its assignment as a specific transition.

It should be noted that the optical properties of the crystal require that polarized light be propagated with the $\vec{E}$ vector along certain crystal axes to avoid rotation of the plane of polarization.[6] These directions are defined by crystal symmetry and are listed in Table III-1. Thus, the polarized molecular absorption spectrum is obtained from the square of the projections [see Eq. (III-1b)] of the $\vec{E}$ vector onto the molecular axes which are known from the crystal structure.

The polarized single crystal absorption spectrum of D_{2d}–$CuCl_4^=$ is given[7] in Figure III-4. When the $\vec{E}$ vector of light is oriented along the molecular z axis, an absorption band is observed[8b] at ~9400 cm^{-1}. From the selection rules given at the bottom of Figure III-3, this absorption band can be assigned as the ${}^2B_2 \rightarrow {}^2A_1$ transition. For $\vec{E}$ oriented along the x,y molecular axes a band is observed at ~5500 cm^{-1} which can then be definitively assigned as the ${}^2B_2 \rightarrow$

TABLE III-1
Optical properties of crystals for polarized spectroscopy

Optical properties	Crystal symmetry	Symmetry defined directions
Isotropic	Cubic	Unpolarized
Uniaxial	Trigonal	$E \parallel + \perp C_3$
	Tetragonal	$E \parallel + \perp C_4$
	Hexagonal	$E \parallel + \perp C_6$
Biaxial	Orthorhombic	$E \parallel + \perp 3\ C_2$'s
	Monoclinic	$E \parallel + \perp C_2$
	Triclinic	No symmetry defined direction

^2E transition. The $^2B_2 \rightarrow {}^2B_1$ transition of $CuCl_4^=$ is forbidden in the D_{2d} geometry. However, the actual symmetry at the copper site in the crystal is C_s, and this, combined with the effects of spin-orbit coupling, makes this transition observable as a weak band[8b] at ~8000 cm^{-1} (not shown in Figure III-4).

C. Comparison of Experiment and Theory

Polarized single crystal absorption spectroscopy has enabled the definitive assignment of the ligand-field absorption spectrum of $CuCl_4^=$ in both the D_{4h} and the D_{2d} distorted tetrahedral geometries.[8b,9] These assignments are summarized in Figure III-5. Clearly the intensity of the $d \rightarrow d$ transitions increase by about an order of magnitude with a static noncentrosymmetric D_{2d} distortion as discussed in Section III-A. Further, the $d \rightarrow d$ transition energies decrease significantly as the complex is distorted from square planar toward tetrahedral. Thus, the ligand-field transitions are particularly powerful probes of the geometry of the metal complex.

The definitive nature of the data in Figure III-5a allows an experimental evaluation of the accuracy of ligand-field theory, at least with respect to its ability to predict changes in transition energy with changes in geometry for fixed ligation.[10] A number of $CuCl_4^=$ complexes have been structurally characterized. Depending on the counter-ion, these have geometries which cover a large range of distortions from D_{2d} to D_{4h} $CuCl_4^=$. The data at the top of Figure III-5a is that of Cs_2CuCl_4 which is close to the tetrahedral limit. These experimental transition energies are plotted as points in Figure III-5b (indicated by the dashed arrow at the appropriate geometry)

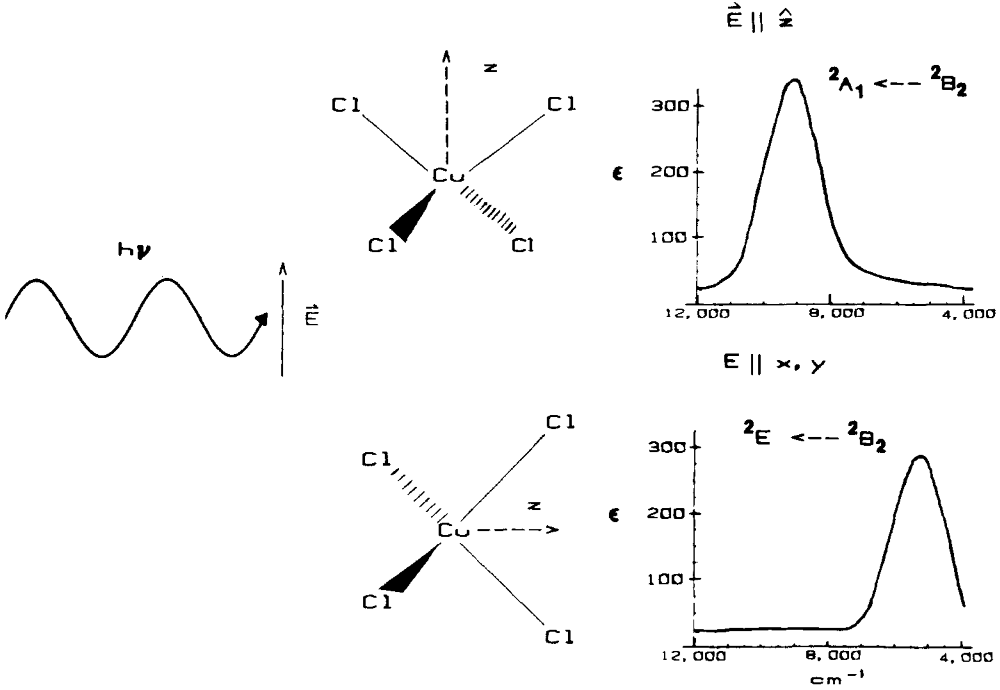

FIGURE III-4 Polarized single crystal absorption spectra of D_{2d}–CuCl$_4^=$: $\vec{E}$ parallel (top) and perpendicular (bottom) to the molecular *z* axis (adapted from Ref. 8b; see Ref. 7).

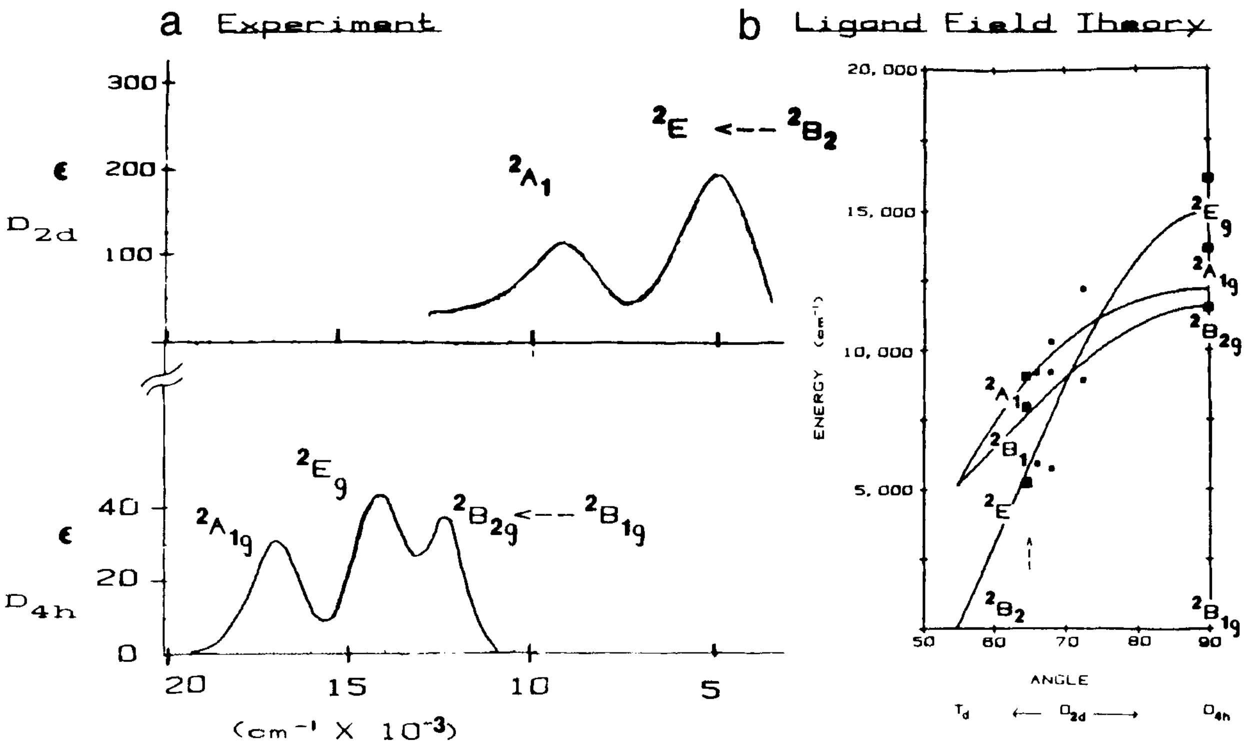

FIGURE III-5 Spectral assignments and ligand field theory of D_{2d}– and D_{4h}–$CuCl_4^{=}$: (a) unpolarized spectra (adapted from Refs. 8b and 9). (b) Ligand-field calculations and spectra from a series of $CuCl_4^{=}$ salts for distortion from T_d to D_{4h}–$CuCl_4^{=}$.

along with data from other $CuCl_4^=$ complexes with increasing distortion toward the square planar limit. The data in Figure III-5a, bottom, for the *N*-methylphenethylammonium salt of $CuCl_4^=$ is plotted at the D_{4h} limit in Figure III-5b. The transition energies of Cs_2CuCl_4 were fit to obtain parameters for a ligand-field calculation for this D_{2d} geometry. From Figure III-5b, extrapolation of this D_{2d} ligand-field calculation toward the D_{4h} geometry clearly predicts the correct general trends in increasing transition energies and there is some quantitative agreement with experiment. However, this ligand-field calculation only takes into account the effects of variation of geometry within the *d* orbitals; yet variations in mixing with other orbitals can also occur. Thus, while the ligand-field calculation predicts the $^2B_{1g} \rightarrow {}^2E_g$ transition to be at highest energy in D_{4h}, experimentally the highest energy transition in D_{4h} must be assigned[9] as $^2B_{1g} \rightarrow {}^2A_{1g}$. If a ligand-field calculation is extended[9,11] to include ~5% Cu 4*s* mixing into the $3d_{z^2}$ orbital (i.e., both have the same symmetry in D_{4h}) by the square planar ligand field, the energy of the $^2B_{1g} \rightarrow {}^2A_{1g}$ transition is raised enough to agree with experiment. Alternatively, SCF-Xα-SW calculations[12] directly give the $^2B_{1g} \rightarrow {}^2A_{1g}$ transition to be at highest energy.

References

1. (a) D. S. McClure, *Electronic Spectra of Molecules and Ions in Crystals* (Academic Press, New York, 1959).
   (b) J. Ferguson, Prog. Inorg. Chem. **12**, 159 (1970).
   (c) A. B. P. Lever, *Inorganic Electronic Spectroscopy* (Elsevier, New York, 1968).
2. A. S. Davydov, *Quantum Mechanics* (NEO Press, Ann Arbor, 1966).
3. C. J. Ballhausen, *Introduction to Ligand Field Theory* (McGraw-Hill, New York, 1962).
4. F. A. Cotton, *Chemical Applications of Group Theory*, 2nd ed. (Wiley-Interscience, New York, 1971).
5. Note that an odd parity perturbed ground state ψ_g' must also be considered in parallel to Eq. (III-3), but with a larger energy denominator.
6. R. E. Stoiber and S. A. Morse, *Microscopic Identification of Crystals* (Ronald Press Company, New York, 1972).
7. The spectrum in Figure III-4 was estimated by correlating the solution spectrum (Ref. 8a) to the polarized single crystal spectrum (Ref. 8b) of the *a-b* face of Cs_2CuCl_4 using the molecular projections ($b = x,y$ and $a = 0.638z + 0.362x,y$) and assuming D_{2d} effective site symmetry (molecular $x = y$).
8. (a) C. Furlani and G. Morpurgo, Theoret. Chim. Acta **1**, 102 (1963).
   (b) J. Ferguson, J. Chem. Phys. **40**, 3406 (1964).
9. M. A. Hitchman and P. J. Cassidy, Inorganic Chemistry **18**, 1745 (1979).

10. E. I. Solomon, J. W. Hare, D. M. Dooley, J. H. Dawson, P. J. Stephens, and H. B. Gray, J. Am. Chem. Soc. **102**, 168 (1980), and references therein.
11. (a) D. W. Smith, Inorg. Chim. Acta **22**, 107 (1977).
(b) M. Gerloch, J. H. Harding, and R. G. Wooley, Struct. Bond. **46**, 1 (1981).
12. S. R. Desjardins, K. W. Penfield, S. L. Cohen, R. L. Musselman, and E. I. Solomon, J. Am. Chem. Soc. **105**, 4590 (1983).

IV. ELECTRONIC ABSORPTION—CHARGE TRANSFER TRANSITIONS

A. Basic Principles

When the absorption spectrum of $CuCl_4^=$ is extended to energies higher than those associated with the $d \rightarrow d$ transitions, new, extremely intense absorption bands are observed. These are Laporté-allowed charge-transfer transitions which result from optical excitation of an electron from the valence $3p$ orbitals on the chloride ligands into the half-occupied $d_{x^2-y^2}$ orbital on the copper ion. Interpretation of the energy and intensity of these ligand-to-metal charge transfer transitions requires that the energy level diagram in Figure III-1 now be extended to include the valence orbitals on the four chloride ligands.

In D_{4h}–$CuCl_4^=$, each chloride ligand donates three $3p$ valence orbitals, one of which participates in a σ type of bonding interaction along the Cl–Cu bond, the other two being perpendicular to the Cl–Cu bond and involved in in-plane-(h) and out-of-plane-(v) π type bonding with the copper (Figure IV-1). Treating the equivalent orbitals on the four Cl^- ligands together, nine different symmetry-adapted linear combinations of ligands orbitals, χ_L, are obtained.[2] These are given in Figure IV-1. In the $CuCl_4^=$ complex these ligand-orbital combinations are split in energy both due to ligand-ligand interactions and bonding interactions of χ_L with metal-centered orbitals of the same symmetry. Consideration of these interactions results in the qualitative molecular-orbital energy level ordering shown in Figure IV-2. The specific order and quantitative splitting of the levels can be very dependent on the type of molecular bonding calculation used. Thus it is critical that the calculated energy level diagram be evaluated experimentally. Excitation of electrons from the filled ligand-centered orbitals into the hole in the copper $d_{x^2-y^2}$ produces the charge-transfer excited states indicated to the right of